*Iranian Journal of Oil & Gas Science and Technology,* Vol. 5 (2016), No. 3, pp. 62-72
http://ijogst.put.ac.ir

# Assessing the Asphaltene Adsorption on Metal Oxide Nanoparticles

**Fatemeh Amin[1] and Ali Reza Solaimany Nazar[2*]**

[1] M.S. Student, Chemical Engineering Department, University of Isfahan, Isfahan, Iran
[2] Associate Professor, Chemical Engineering Department, University of Isfahan, Isfahan, Iran

*Received:* June 28, 2015; *revised:* August 06, 2015; *accepted:* October 26, 2015

## Abstract

The Taguchi design of experiments (DOE) approach is adopted here to evaluate the impact of effective factors such as nanoparticles type, nanoparticles to model solution mass ratio, asphaltene structure, and temperature on asphaltene adsorption equilibrium. Herein, the toluene-asphaltene solution model is applied. Three commercially nanoparticles ($SiO_2$, $Al_2O_3$, and $TiO_2$) are used. Asphaltene characterizations are carried out by X-ray diffraction (XRD) analysis. It is found that the nanoparticle type and asphaltene structure with a respective influence of 48.5% and 3.11% have the maximum and minimum contribution on the amount of adsorbed asphaltene at the selected levels respectively. Aluminum oxide nanoparticle has the maximum and silicon oxide nanoparticle shows the minimum adsorption. The temperature has no statistical significance. Asphaltenes with higher aromaticity have more tendencies for adsorption on nanoparticles.

**Keywords:** Asphaltene, Adsorption, Nanoparticles, Taguchi Design

## 1. Introduction

Crude oil is a colloidal system having a disperse phase composed of asphaltene and resin. Asphaltenes are the fraction of petroleum liquids insoluble in the low-molecular-weight normal paraffins such as the *n*-heptane while soluble in some aromatic solvents such as toluene or benzene (Bouhadda et al., 2007; Nassar, 2010). Asphaltenes are not chemically identifiable compounds. Their composition and structure depend on their source, the method of extraction, and the type of solvents used in extraction (Groenzin, and Mullins, 2000).

Asphaltene can be adsorbed on surfaces as colloidal aggregates. Asphaltene adsorption on various surfaces can cause many problems during heavy oil extraction, transportation, and upgrading (Mochida, 1988). These problems have forced the researchers to employ various surfaces for asphaltene removal through adsorption from crude oil. Surfaces were applied in previous adsorption studies include mineral, metallic, and metal oxide (Alboudwarej, 2005; Marczewski and Szymula, 2002; Rudrake, et al., 2009). Nowadays, the use of nanoparticle metal oxides due to having a big specific surface area is of concern (Nassar, 2010; Franco et al., 2013; Xinhu and Dongyang, 2011). The majority of the previous studies focused on the adsorption isotherms. Nassar investigated the effect of some of the affecting factors on the asphaltene adsorption on nanoparticles like asphaltene initial concentration, nanoparticle type, temperature, nanoparticle size, surface pH, water content, and coexisting molecules (Nassar, 2010; Nassar et al., 2011a,b). Asphaltene adsorption behavior varies on

* Corresponding Author:
Email: asolaimany@eng.ui.ac.ir

different nanoparticles. Researchers have proposed various hypotheses regarding asphaltenes molecules and surface bonding. Gonzalez et al. (2007) concluded that the presence of oxygen and nitrogen in the structure of asphaltenes contributes to the amount adsorbed. Researchers have noted that the polar interaction between the asphaltene molecules and the surface take place during the asphaltene adsorption (Dudasova et al., 2008). According to the introduced hypothesis in the recent studies, the aromaticity of asphaltene and nitrogen content in the asphaltene structure is related to asphaltene adsorption (Lopez-Linares et al., 2009).

Different interactions could occur between surface and asphaltene molecules. Buckley and Liu (1998) reported the main categories of asphaltene/solid interactions as: (1) polar interaction between the polar groups of asphaltenes and the surface, (2) surface precipitation, (3) acid-base interaction at solid/water and asphaltene/water interfaces, and (4) ion bonding and specific interaction. In the absence of water, only the two first categories are involved.

In this study, the influences of effective factors like nanoparticle types, asphaltenes types, the ratio of nanoparticles to asphaltene model solution, and temperature on the amount of asphaltene adsorption on metal oxides nanoparticles are evaluated. Herein, the potential of the asphaltenes extracted from two different crude oil types adsorbed on three types of nanoparticles are measured.

## 2. Experimental methods

### 2.1. Materials

In this study, three commercially available nanoparticles ($SiO_2$, $Al_2O_3$, and $TiO_2$) are provided from TECNAN. The reported particle size and specific surface area are listed in Table 1. The asphaltenes are extracted from two different crude oil types both from the south of Iran. The crude oil samples properties are presented in Table 2. The solvents used in the precipitation and extraction of asphaltene are *n*-heptane and toluene (analytical grade, EMD, Merck, NJ).

**Table 1**
Properties of the applied nanoparticles.

| Nanoparticles | Average particle size[nm] | Specific surface area (BET)[$m^2/g$] |
|---|---|---|
| **$\gamma$-$Al_2O_3$** | 10-20 | 110 |
| **$TiO_2$** | 10-15 | 120 |
| **$SiO_2$** | 10-15 | 199 |

**Table 2**
The selected factors with their levels.

| Factors | Symbol | Level | | |
|---|---|---|---|---|
| **Asphaltene type** | A | Sample 1 | | Sample 2 |
| **Nanoparticle type** | B | $TiO_2$ | $SiO_2$ | $\gamma$-$Al_2O_3$ |
| **Nanoparticles to model solution ratio [l/g]** | C | 1:2 | 1:5 | 1:10 |
| **Temperature [°C]** | D | 25 | 35 | 45 |

## 2.2. Asphaltene extraction and model solution

Residue is extracted from crude oil according to ASTM D86-01; next, the asphaltene is extracted from residues according to ASTM D6560-00. The asphaltene is dissolved in toluene for the preparation of the model solution of asphaltene. The concentration of asphaltene solution in the adsorption experiments is 4000 mg/l.

## 2.3. Asphaltene characterization

Asphaltene characterizations are carried out by X-ray diffraction (XRD) analysis. The XRD measurement is conducted through a Bruker automated diffractometer, applying the CuKα (=1.5406 Å) wavelength. A nickel detector is employed to collect the diffraction signals. The diffraction angle ($2\theta$) is scanned from 5 to 45° at a 0.005 ($2\theta$/sec) scan rate with a 2 (sec/step) step size.

## 2.4. Adsorption experiment

A specific amount of nanoparticles is added to the model solution of asphaltenes in a constant volume (10 ml). The samples are shaken at 300 rpm for 3 hrs at a specified temperature in a shaker incubator (NB-205V, N-Biotek instrument Korea, Inc.) in order to achieve adsorption equilibrium. Next, the samples are centrifuged (Supra 22K, Hanil instrument Korea, Inc.) for 15 min at 5000 rpm to remove the suspended nanoparticles. The concentrations of the nanoparticles in the supernatant are determined using an atomic emission spectroscopy. The results indicate that all of the nanoparticles are separated by centrifugation. Asphaltene concentration in the supernatant is determined by an UV-visible spectrophotometer (V570, Jasco instrument USA, Inc.). A calibration curve of UV-visible absorbance at ~800 nm is obtained using standard model solutions with known asphaltene concentrations versus the asphaltene concentration (Marczewski and Szymula, 2002; Evdokimov et al., 2003). The adsorption of asphaltene on the nanoparticles is evaluated by measuring the asphaltene concentration in the solution before and after mixing them with nanoparticles. The amount of asphaltenes adsorbed after obtaining adsorption equilibrium, $q_e$ (mg/m$^2$), is calculated through the following equation:

$$q_e = \frac{C_e - C_0}{A \times m} V \tag{1}$$

where, $V$ is the sample volume (l); $m$ is the mass of the nanoparticles (gr); $A$ is the nanoparticle specific surface area (m$^2$/g); $C_o$ is the initial concentration of asphaltenes in the solution (mg/l) and $C_e$ is the asphaltene concentration in the solution after adsorption equilibrium (mg/l).

## 2.5. Design of experiments (DOE)

The conventional approach for evaluating the effect of the factors in the response of the system is the one-factor-at-a-time method. When the factors are numerous, this approach requires many experimental runs. DOE is a statistical technique used in studying multiple factors simultaneously. DOE can reduce the number of experiments while retaining the quality of data collection. The first important step in DOE is the selection of suitable factors and their levels. In this study, the four factors, namely nanoparticle type, asphaltenes structure, ratio of nanoparticles to model solution, and temperature, are considered with their levels presented in Table 3. The Taguchi method is one of the most reliable methods adopted for the design of experiments. For the Taguchi approach with the selected factors in this experiment an $L_{18}$ non-orthogonal array is designed by the statistical

MINITAB® software release 14 (Minitab Inc.) (Table 4). Each row of the matrix represents one run in a specified condition. In order to avoid the systematic bias, the sequence, in which these runs are made, is randomized (Roy, 2001). All analyses are performed on a modified response signal-to-noise ratio (*S/N*). The *S/N* in the Taguchi method indicates the magnitude of changes in the response due to the variations of controlled factors with respect to that of the errors. As mentioned above, the results obtained from the adsorption of asphaltenes on nanoparticles are applied to the response analysis. In order to maximize the amount of the adsorption of asphaltene on nanoparticles, the following *S/N* equation is applied (Roy, 2001):

$$S/_N = -10Log(\frac{\sum 1/Y^2}{n}) \quad (2)$$

**Table 3**

$L_{18}$ Taguchi non-orthogonal array of the designed experiments based on the natural variables and converted response on S/N ratio.

| Run | A | B | C | D | *S/N* ratio |
|---|---|---|---|---|---|
| **1** | 1 | $TiO_2$ | 1:2 | 25 | 2.66 |
| **2** | 1 | $TiO_2$ | 1:5 | 35 | 3.99 |
| **3** | 1 | $TiO_2$ | 1:10 | 45 | 5.49 |
| **4** | 1 | $SiO_2$ | 1:2 | 25 | -0.29 |
| **5** | 1 | $SiO_2$ | 1:5 | 35 | 1.71 |
| **6** | 1 | $SiO_2$ | 1:10 | 45 | 2.66 |
| **7** | 1 | $Al_2O_3$ | 1:2 | 35 | 3.58 |
| **8** | 1 | $Al_2O_3$ | 1:5 | 45 | 5.31 |
| **9** | 1 | $Al_2O_3$ | 1:10 | 25 | 7.58 |
| **10** | 2 | $TiO_2$ | 1:2 | 45 | 3.41 |
| **11** | 2 | $TiO_2$ | 1:5 | 25 | 6.18 |
| **12** | 2 | $TiO_2$ | 1:10 | 35 | 7.55 |
| **13** | 2 | $SiO_2$ | 1:2 | 35 | -1.68 |
| **14** | 2 | $SiO_2$ | 1:5 | 45 | 1.84 |
| **15** | 2 | $SiO_2$ | 1:10 | 25 | 4.93 |
| **16** | 2 | $Al_2O_3$ | 1:2 | 45 | 3.66 |
| **17** | 2 | $Al_2O_3$ | 1:5 | 25 | 6.96 |
| **18** | 2 | $Al_2O_3$ | 1:10 | 35 | 8.88 |

where, *Y* is the experimental measurement of the adsorption of asphaltene from model solution, and *n* is the number of replications, presented herein as *n*=2.

## 3. Results and discussions

### 3.1. Asphaltene characterization

The X-ray patterns of both samples are shown in Figure 1. The characteristic values are obtained from X-ray patterns of the extracted asphaltenes samples and summarized in Table 5. The aromaticity ($f_a$) is the aromatic hydrocarbons to all hydrocarbons (aromatic and saturated hydrocarbon) content ratio. The aromaticity $f_a$ was determined by calculating the areas *A* of the peaks for the $\gamma$ and the graphene bands using the following formula reported in the literature (Solaimany Nazar, and Bayandory, 2005):

$$f_a = \frac{C_A}{C_A + C_S} = \frac{A_{graphene}}{A_{graphene} + A_\gamma} \tag{3}$$

where, $C_A$ and $C_S$ are the number of saturated and aromatic carbon atoms per structural unit respectively. The γ and the graphene curves which are extracted from the X-ray patterns of the Samples 1 and 2 are presented in Figures 2 and 3 respectively.

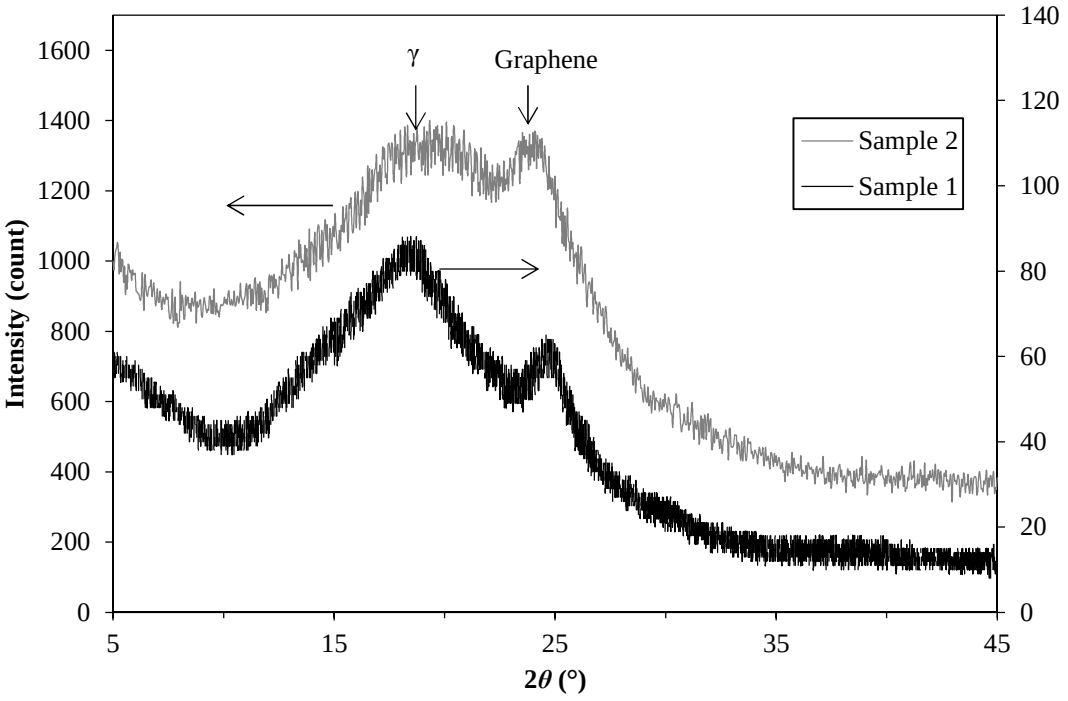


**Figure 1**
X-ray diffraction patterns of two Iranian crude asphaltene samples.

The layer distance between aromatic sheets ($d_m$) is calculated from the maximum of the graphene band by the Bragg relation. Distance between aliphatic layers is presented as $d_\gamma$. The average height of the stack of aromatic sheets perpendicular to the plane of the sheet ($L_c$) is calculated from the graphene curve. The number of aromatic sheets in a stacked cluster, *M*, is estimated from the values of the $L_c$ and $d_m$. All the terms are determined through the formula presented by Refs. (Bouhadda et

al., 2007; Shirokoff et al., 1997). More details on the asphaltene characterizations by X-ray diffraction (XRD) analysis are presented elsewhere (Solaimany Nazar, and Bayandory, 2005). The aromaticity of the extracted asphaltene type 2 is greater than that of the extracted asphaltene type 1. The aromaticity value indicates that the extracted asphaltene type 2 is more polar than the type 1 (Long, 1981).

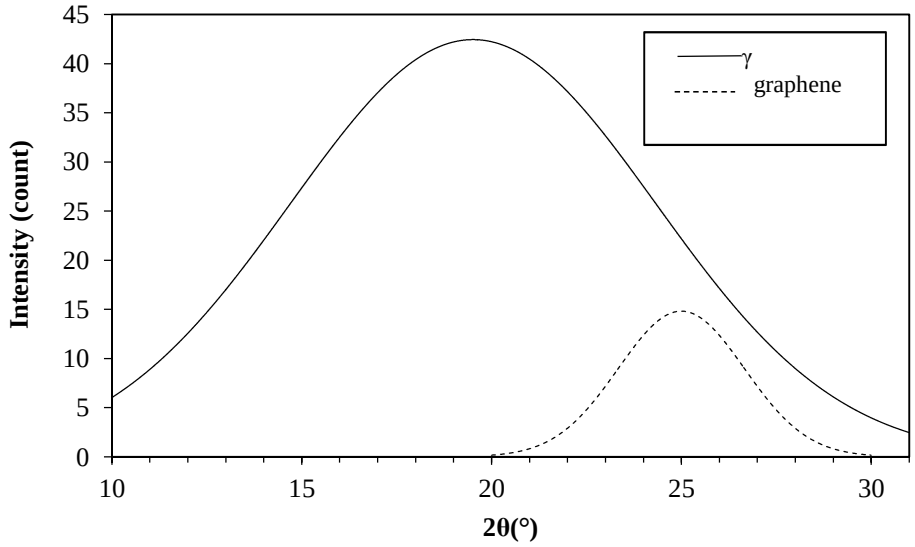


**Figure 2**
The γ and graphene curves extracted from XRD pattern of asphaltene Sample 1.

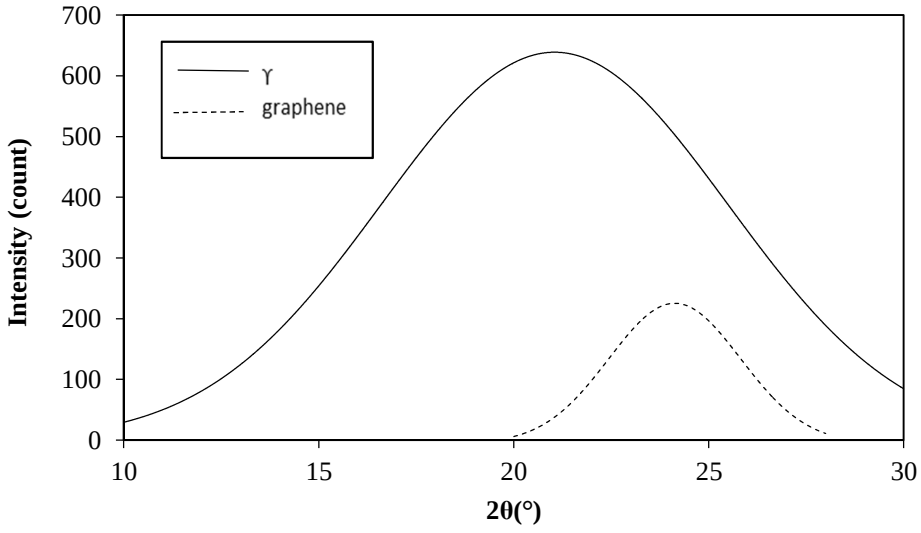


**Figure 3**
The γ and graphene curves extracted from XRD pattern of asphaltene Sample 2.

## 3.2. Analysis of variance (ANOVA)

The corresponding *S/N* ratios of all the 18 response runs with their replication are presented in Table 4. The ANOVA approach is adopted in the Taguchi method to determine the key factors and influences, interactions, and errors. The strategy of ANOVA calculation is to analyze the variation

that each factor cause relative to the total variation observed in the results statistically (Montgomery, 1997). The statistical analysis of the results is obtained through MINITAB® release 14 (Minitab Inc.) software. ANOVA statistical terms and the percentage of the contribution of each factor are presented in Table 6. In the ANOVA table, the *F*-ratio is an important term, which is applied in the calculation of the effect of a factor and the variance influenced by the error term. Comparing the *F*-ratio of the factor obtained in the analysis with a critical *F*-ratio ($F_c$ = 4.96 for factors with two levels, $F_c$ = 4.1 for factors with 3 levels) with a confidence level of 95% (Roy, 2001) indicates whether that factor has a significant influence on the response. It should be emphasized that the interpretation of ANOVA table is valid just in the range of levels considered for any specific factor. In this study, it is obvious from *F*-ratios, that the three selected factors in the selected range considered in the experimental design have a statistically significant effect at a 95% confidence level. The temperature has no significant effect on the response in the selected levels. The residual error term combines the effects of the three sources: factors excluded from the experiment, uncontrollable factors, and experimental error (Roy, 2001).

**Table 4**
Structural parameters deduced from X-ray diffraction for two samples asphaltenes.

| Sample | $f_a$ | $D_m$(Å) | $d_\gamma$(Å) | $L_c$(Å) | *M* |
|---|---|---|---|---|---|
| **1** | 0.11 | 3.55 | 4.58 | 20.9 | 6.8 |
| **2** | 0.12 | 3.68 | 4.21 | 26.1 | 8.1 |

**Table 3**
Analysis of variance (ANOVA).

| Source | Degree of freedom (DOF) | Sum of squares (SS) | Variance | *F*-ratio | Pure sum | Percent influence |
|---|---|---|---|---|---|---|
| **A** | 1 | 4.531 | 4.531 | 10.74 | 0.008 | 3.11 |
| **B** | 2 | 64.960 | 32.48 | 77.01 | 0.000 | 48.5 |
| **C** | 2 | 55.628 | 27.81 | 65.95 | 0.000 | 41.5 |
| **D** | 2 | 2.807 | 1.40 | 3.33 | 0.078 | 1.48 |
| **Residual error** | 10 | 4.218 | 0.4218 | | | 5.4 |
| **Total** | 17 | 132.143 | | | | 100 |

## 3.3. The effect of nanoparticle type

The results of experimental design indicate that the adsorbent type, with a 48.5% influence obtained from ANOVA, is the most important factor with the greatest impact on the amount of asphaltene adsorbed on the nanoparticle surfaces. The effect of the different nanoparticles on asphaltene adsorption is shown in Figure 4. Aluminum oxide nanoparticle has the maximum and silicon oxide nanoparticle has the minimum adsorption. Adsorption depends on the interaction between the adsorbent and the adsorbed liquid, so these differences in the amount of adsorption can be attributed to a degree of difference in the interaction between metal oxide surface and the asphaltenes. Similar observations were reported by other researchers for the adsorption of asphaltenes on different surfaces (Alboudwarej, 2005; Nassar et al., 2011c). The hydrophobicity of surface can change the mechanism of adsorption and have an effect on asphaltene adsorption (Dudasova et al., 2008). The pH of the

adsorbent surface has an influence on asphaltene adsorption. The acidic surface was shown to have the highest adsorption (Nassar et al., 2011a).

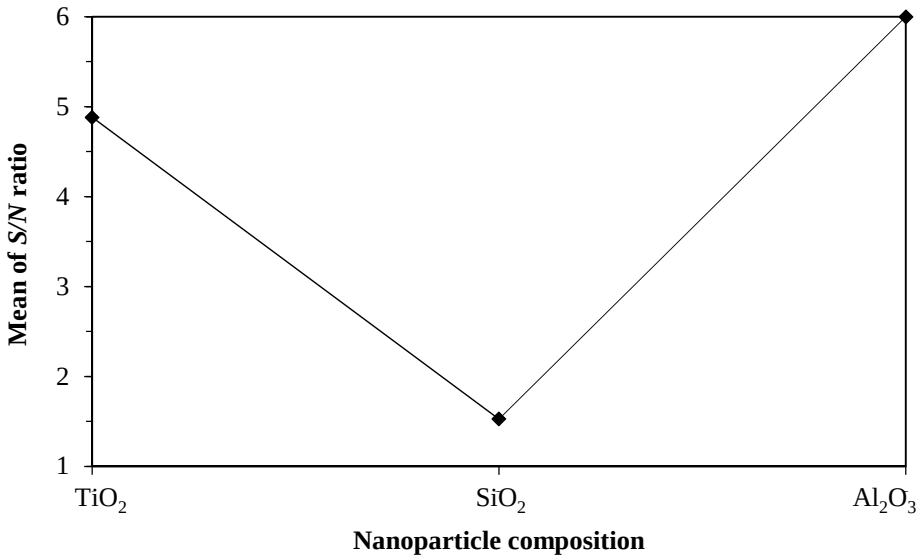


**Figure 4**
Main effect plot of the nanoparticle composition on S/N ratio for asphaltene adsorption.

## 3.4. The effect of nanoparticle to model solution mass ratio

An increase in the amount of adsorbent leads to an increase in the adsorption sites, which causes an increase in the adsorption of asphaltene. The effect of the adsorbent addition is shown in Figure 5. In the selected levels, the amount of asphaltene adsorption increases linearly with an increase in the adsorbent amount. It is clear that beyond a certain amount of adsorbent, adding more adsorbent has no impact on the asphaltene adsorption amount.

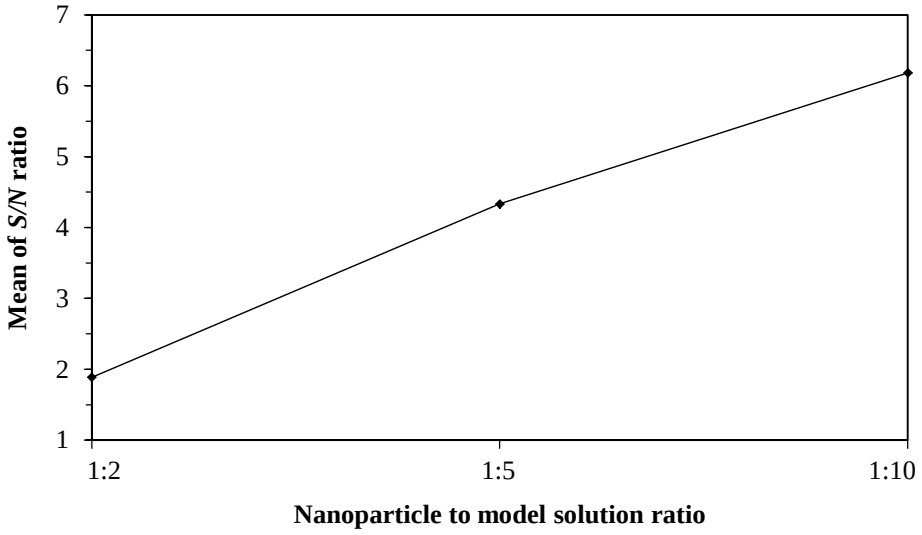


**Figure 5**
Main effect plot of the nanoparticle to model solution ratio on S/N ratio for asphaltene adsorption.

### 3.5. The effect of asphaltene structure on adsorption

Asphaltene has no specific chemical structure and any change in its structural parameters would affect its adsorption on nanoparticles. The effect of asphaltene structure is shown in Figure 6. In this study, the two asphaltene samples have many structural similarities. Therefore, the percent influence of asphaltene structure is less than the other two mentioned factors. The adsorption amount of type 2 asphaltene is more than that of the type 1 asphaltene, which could be due to the higher aromaticity of type 2. It is expected that by using asphaltene samples with more structural differences, a more noticeable influence on the adsorption in ANOVA table could be evaluated.

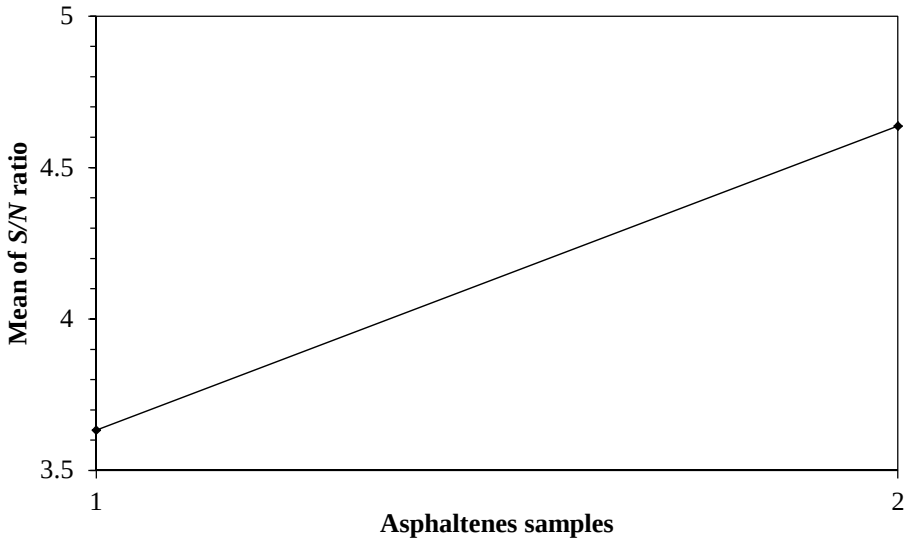


**Figure 6**
Main effect plot of the asphaltene samples on S/N ratio for asphaltene adsorption.

According to the characterization of asphaltene samples, it is found that the aromaticity of Sample 2 is more than Sample 1. Leon et al. reported that the asphaltenes with more aromaticity have more adsorption (Leon et al., 2000). Increasing the aromaticity and polarity of asphaltene can cause an increase in polar interaction between the polar groups of asphaltene and the adsorbent surface; hence, an increase in the amount of asphaltene adsorption is seen.

## 4. Conclusions

Asphaltene removal through adsorption from crude oil by employing various metal oxide nanoparticles is a new challenge in heavy oil recovery investigation. The potential of the asphaltenes adsorption on three types of nanoparticles are measured. The influence of various effective factors on the asphaltene adsorption is analyzed using the Taguchi experimental approach statistically. The *F*-ratios of the factors like asphaltene structure, nanoparticles type, and nanoparticle to model solution mass ratio indicate a statistical significance. The temperature has no significant impact over the range of 25 to 45 °C. It is found that the nanoparticle type has the maximum and asphaltene structure shows the minimum percentages of contribution to the asphaltenes adsorption. Asphaltene with a higher aromaticity could lead to a more asphaltene adsorption on nanoparticles. The possibility of heavy oil upgrading in the presence of nanoparticles through asphaltene catalytic oxidation reactions is purposed for further study.

## Nomenclature

| | |
|---|---|
| $A$ | : Area of the peak for the γ or the graphene bands |
| ANOVA | : Analysis of variance |
| $C_A$ | : Number of aromatic carbon atoms per structural unit |
| $C_S$ | : Number of saturated carbon atoms per structural unit |
| $d_m$ | : Layer distance between aromatic sheets |
| DOE | : Design of experiments |
| $d_\gamma$ | : Distance between aliphatic layers |
| $f_a$ | : Aromaticity |
| $L_c$ | : Average height of the stack of aromatic sheets perpendicular to the plane of the sheet |
| $M$ | : Number of aromatic sheets in a stacked cluster |
| $n$ | : Number of replications |
| $Y$ | : Experimental measurement value of the adsorption of asphaltene |

## References

Alboudwarej, H., Pole, D., Svrcek, W. Y., and Yarranton, H. W., Adsorption of Asphaltenes on Metal, Industrial and Engineering Chemistry Research, Vol. 44, No. 15, p. 5585-5592, 2005.

Bouhadda, Y., Bormann, D., Sheu, E., Bendedouch, D., Krallafa, A., and Daaou, M., Characterization of Algerian Hassi-Messaoud Asphaltene Structure Using Raman Spectrometry and X-ray Diffraction, Fuel, Vol. 86, No. 12-13, p. 1855-1864, 2007.

Buckley, J. S. and Liu, Y., Some Mechanisms of Crude Oil/Brine/Solid Interactions, Journal of Petroleum Science and Engineering, Vol. 20, No. 3-4, p.155-160, 1998.

Dudasova, D., Simon, S., Hemmingsen, P. V., and Sjoblom, J., Study of Asphaltenes Adsorption onto Different Minerals and Clays: Part 1, Experimental Adsorption with UV Depletion Detection, Colloids and Surfaces A: Physicochemical and Engineering Aspects, Vol. 317, No. 1-3, p.1-9, 2008.

Evdokimov, I. N., Eliseev, N. Y., and Akhmetov, B. R., Assembly of Asphaltene Molecular Aggregates as Studied by Near-UV/Visible Spectroscopy I, Structure of the Absorbance Spectrum, Journal of Petroleum Science and Engineering, Vol. 37, No. 3, p. 135-143, 2003.

Franco, C., Patino, E., Benjumea, P., Ruiz, M. A., and Cortes, F. B., Kinetic and Thermodynamic Equilibrium of Asphaltene Sorption onto Nanoparticles of Nickel Oxide Supported on Nanoparticulated Alumina, Fuel, Vol. 105, p. 408-414, 2013.

Gonzalez, M. F., Stull, C. S., Lopez-Linares, F., and Almao, P. P., Comparing Asphaltene Adsorption with Model Heavy Molecules over Macroporous Solid Surfaces, Energy and Fuels, Vol. 21, No. 1, p. 234-241, 2007.

Groenzin, H. and Mullins, O. C., Molecular Size and Structure of Asphaltenes from Various Sources, Energy and Fuels, Vol. 14, No. 3, p. 677-684, 2000.

Leon, O., Rogel, E., Espidel, J., and Torres, G., Asphaltenes Structural Characterization, Self-Association, and Stability Behavior, Energy and Fuels, Vol. 14, No. 1, p.6-10, 2000.

Long, R. B., The Concept of Asphaltenes, in: Li, N., and Bunger, J. W., Editors, Chemistry of Asphaltenes, Washington DC, American Chemical Society, 1981.

Lopez-Linares, F., Carbognani, L., Sosa-Stull, C., Almao, P. P., and Spencer, R. J., Adsorption of Virgin and Broken Residue Asphaltenes over Solid Surfaces,1. Kaolin, Smectite Clay Minerals, and Athabasca Siltstone, Energy and Fuels, Vol. 23, No. 4, p. 1901-1908, 2009.

Marczewski, A. W. and Szymula, M., Adsorption of Asphaltenes from Toluene on Mineral Surface, Colloids and Surfaces A: Physicochemical and Engineering Aspects, Vol. 208, No. 1-3, p.259-266, 2002.

Mochida, I., Zhao, X., and Sakanishi, K., Catalyst Deactivation During the Hydrotreatment of Asphaltene in an Australian Brown Coal Liquid, Fuel, Vol. 67, No. 8, p.1101-1105, 1988.

Montgomery, D. C., Design and Analysis of Experiments, 4th Edition New York, Wiley, 1997.

Nassar, N. N., Asphaltene Adsorption onto Alumina Nanoparticles: Kinetics and Thermodynamic Studies, Energy and Fuels, Vol. 24, No. 8, p. 4116-4122, 2010.

Nassar, N. N., Hassan, A., and Almao, P. P., Effect of Surface Acidity and Basicity of Aluminas on Asphaltene Adsorption and Oxidation, Journal of Colloid and Interface Science, Vol. 360, No. 1, p. 233-238, 2011a.

Nassar, N. N., Hassan, A., and Almao, P. P., Effect of Particle Size on Asphaltene Adsorption and Catalytic Oxidation onto Alumina Nanoparticle, Energy and Fuels, Vol. 25, No. 9, p. 3961-3965, 2011b.

Nassar, N. N., Hassan, A., and Almao, P. P., Metal Oxide Nanoparticles for Asphaltene Adsorption and Oxidation, Energy and Fuels, Vol. 25, No. 3, p. 1017-1023, 2011c.

Roy, R., Design of Experiments Using the Taguchi Approach, New York, Wiley, 2001.

Rudrake, A., Karan, K., and Horton, J. H., A Combined QCM and XPS Investigation of Asphaltene Adsorption on Metal Surfaces, Journal of Colloid and Interface Science, Vol. 332, No. 1, p. 22-31, 2009.

Shirokoff, J. W., Siddiqui, M. N., and Ali, M. F., Characterization of the Structure of Saudi Crude Asphaltenes by X-ray Diffraction, Energy and Fuels, Vol. 11, No. 3, p. 561-565, 1997.

Solaimany Nazar, A. R. and Bayandory, L., Investigation of Asphaltene Stability in the Iranian Crude Oils, Iranian Journal of Chemical Engineering, Vol. 5, No. 1, p. 3-12, 2005.

Xinhu, T. and Dongyang, L., Evaluation of Asphaltene Degradation on Highly Ordered $TiO_2$ Nanotubular Arrays via Variations in Wettability, Langmuir, Vol. 27, p. 1218-1223, 2011.